N-63-4-3

R 242

Technical Report

LOW-FREQUENCY SHIELDING EFFECTIVENESS OF CONDUCTIVE GLASS

20 May 1963

U. S. NAVAL CIVIL ENGINEERING LABORATORY
Port Hueneme, California

LOW-FREQUENCY SHIELDING EFFECTIVENESS OF CONDUCTIVE GLASS

Y-F006-09-206

Type C

by

H. A. Lasitter

ABSTRACT

The shielding effectiveness of conductive glass at low and intermediate frequencies (100 kc to 1,000 mc) was investigated. A mathematical model was used to describe the absorption and reflection. This model is based on a film applied to the glass substrate which represents a barrier with finite thickness and relative conductivity. Experimental data agreed well with theoretical calculations. Coated glass exhibits a permeability similar to that of free space, so that low-impedance attenuation is limited to the conductivity of the film. The analysis is primarily concerned with high-impedance, near-field incident waves. Transmission in the visible spectrum was also determined for several 4- by 4-inch conductive glass samples which vary in surface resistance from 9 to 125 ohms/square. Larger samples (8 by 3 feet) of conductive glass were also investigated.*

* Supplement to TR-242, For Official Use Only, lists types of glass related to manufacturers.

INTRODUCTION

In the construction of electromagnetic-interference-shielded buildings, it has been customary to have only one major opening, i.e., an entrance. Heretofore most EMI-shielded enclosures have been a small area with roof, floor, and walls securely bonded so that leakage in the region 14 kc to 1,000 mc is negligible. An enclosure of this type can offer attenuations on the order of 90-100 db, depending on (1) the material the walls are made of; (2) how well the entrance-exit is sealed; and (3) how well the enclosure is constructed. For limited areas this approach is satisfactory and good shielding integrity can be maintained.

For larger buildings, however, the cost of such a structure is prohibitive and cheaper methods need to be investigated. In particular, if 90- to 100-db isolation is not the most stringent requirement, then cheaper methods can be used. In addition, it becomes feasible to improve the asthetic qualities of a building by incorporating windows in a normally windowless structure. Windows would provide important, though subtle, psychological benefits for personnel inside the building. The use of commercially available conductive glass has been suggested for use with buildings where a lesser degree of shielding is required.

This report investigates the shielding qualities of large panes of conductive glass to be used in conjunction with buildings offering a degree of EMI shielding and other shielding applications where visibility is required. Theoretical calculations of shielding effectiveness indicate close agreement with experimental data at low and intermediate frequencies. The mathematical calculations are carried out in Appendix A. Samples of conductive glass with surface resistivities (see Appendix B) ranging from 9 to 125 ohms/square, from three manufacturers, were evaluated, and data is presented for each surface resistance measured. Three sizes of glass were measured to determine their shielding effectiveness: 4 by 4 inch, 12 by 33 inch, and 3 by 8 feet. The light-transmission qualities of samples of different resistivity were measured and are presented graphically.

Primarily, high-impedance electric fields were chosen for investigation because the conductive coating exhibits a permeability comparable to that of free space although, because of the conductivity, some shielding to low-impedance fields is realized. Measurements of one sample are given for magnetic (low-impedance) fields.

CONTENTS

INTRODUCTION

In the construction of electromagnetic-interference-shielded buildings, it has been customary to have only one major opening, i.e., an entrance. Heretofore most EMI-shielded enclosures have been a small area with roof, floor, and walls securely bonded so that leakage in the region 14 kc to 1,000 mc is negligible. An enclosure of this type can offer attenuations on the order of 90-100 db, depending on (1) the material the walls are made of; (2) how well the entrance-exit is sealed; and (3) how well the enclosure is constructed. For limited areas this approach is satisfactory and good shielding integrity can be maintained.

For larger buildings, however, the cost of such a structure is prohibitive and cheaper methods need to be investigated. In particular, if 90- to 100-db isolation is not the most stringent requirement, then cheaper methods can be used. In addition, it becomes feasible to improve the asthetic qualities of a building by incorporating windows in a normally windowless structure. Windows would provide important, though subtle, psychological benefits for personnel inside the building. The use of commercially available conductive glass has been suggested for use with buildings where a lesser degree of shielding is required.

This report investigates the shielding qualities of large panes of conductive glass to be used in conjunction with buildings offering a degree of EMI shielding and other shielding applications where visibility is required. Theoretical calculations of shielding effectiveness indicate close agreement with experimental data at low and intermediate frequencies. The mathematical calculations are carried out in Appendix A. Samples of conductive glass with surface resistivities (see Appendix B) ranging from 9 to 125 ohms/square, from three manufacturers, were evaluated, and data is presented for each surface resistance measured. Three sizes of glass were measured to determine their shielding effectiveness: 4 by 4 inch, 12 by 33 inch, and 3 by 8 feet. The light-transmission qualities of samples of different resistivity were measured and are presented graphically.

Primarily, high-impedance electric fields were chosen for investigation because the conductive coating exhibits a permeability comparable to that of free space although, because of the conductivity, some shielding to low-impedance fields is realized. Measurements of one sample are given for magnetic (low-impedance) fields.

THEORETICAL CONSIDERATIONS

The shielding properties of conductive glass have been investigated by Hawthorne, et al.[1,2] These references present a theoretical and limited experimental treatment on the basis that the glass and conductive film represent sections of a lossy transmission line and that the incident wave had originated in the far field; hence it was essentially a plane wave by the time the film surface was reached. This theoretical treatment is adequate for frequencies greater than 600 mc/sec (for usual glass thickness), but at lower frequencies the dominant field is induced rather than radiated.

At low frequencies the shielding effectiveness (SE) was evaluated by treating the film as a metallic barrier with an absorption value related to the thickness of the film and a reflection value that is dependent upon the film conductivity, σ_f, and the nature of the incident wave. In addition, both the absorption and reflection are frequency-dependent.

The agreement of the mathematical model for the shielding effectiveness with the experimental data obtained is shown in Figure 1. The decrease of SE for increasing surface resistance, R_s, can be predicted theoretically by using the term $-20 \log_{10} (fr R_s)$ which appears in Equation 46 (Appendix A). Doubling the value of R_s yields a 6-db decrease in SE. This variation in SE was determined experimentally with samples of the conductive glass. Figure 2 shows this experimentally determined decrease in SE for an increase in R_s.

There are practical limits to the value of R_s. These limits are determined primarily by the light-transmission qualities. As R_s decreases, the transmission in the visible region also decreases. The ultimate selection of a conductive glass will depend upon a compromise between the surface resistance and the light transmission required. Samples were obtained that had a value of 9 ohms/square; it is now possible to obtain samples as low as 2 ohms/square. The light transmission for a 2-ohm/square sample is on the order of 50 percent or less. The largest value of R_s obtainable as a commercial glass product is about 1-5 megohms/square. The SE for these higher values is very low; however, the SE for an uncoated sample (indicated by $R_s = \infty$) was determined and is indicated later in the report.

EVALUATION OF SMALL SAMPLES

The experimental test setup is shown in Figure 3. The SE for the samples was determined by the solution of the equation $SE = 20 \log_{10} (E_1/E_2)$ where the voltage measured is E_1 when the sample is not present and E_2 when the sample is inserted.

(This technique is used to determine the SE of any material[3] and is not necessarily restricted to conductive glass.) The only precaution necessary is that the film make good electrical contact with the cavities. A metallic gasket material was placed on the cavities; the gasket then made contact with a fired conductive bus bar on the periphery of the glass sample.

To determine SE (see Figure 3):

1. A signal at the desired frequency was fed into cavity #1. A spacer was placed along the edges of the cavity so that the equivalent spacing of the glass sample was maintained. A direct signal was then available to the detector.

2. The local oscillator was set at the proper frequency so that a maximum was obtained on the indicator. The matching network was then peaked to indicate resonance of the tuned circuit.

3. The attenuator was then increased until the indicator showed some arbitrary level; this level was recorded, representing E_1 in db.

4. The sample was inserted in place of the spacer and the attenuator was shifted until the same indicated level was reached as established in step 3. The new setting of the attenuator represented E_2 in db. The SE was then obtained by subtracting E_1 (db) - E_2 (db).

In addition to the above, preliminary tests were made to determine the magnitude of the signal that "leaked" directly from the generator to the detector. This was accomplished by inserting an aluminum plate of the proper thickness in place of the sample. Over the frequency range covered by the tests, the signal level from leakage was within a few db of the inherent noise level of the detector.

The maximum value of SE that can be measured with this technique is limited in two respects. (SE_{max} occurs when E_1 is as large as possible and E_2 is as small as possible, thus making the difference large.) The first limitation is that the coupling efficiency between the two short probes is extremely poor. This difficulty can be overcome to a certain extent using a generator with higher outputs and/or matching networks between the generator and the probe. The other limitation on SE_{max} is the noise level of the detector. The minimum value of E_2 is determined (in the case of very low leakage) primarily by this noise level. In all the tests the SE_{max} that could be measured was $\leq$ 106 db.

For frequencies between 500 kc and 25 mc the local oscillator, crystal mixer, and IF amplifier shown in Figure 3 were replaced by the AN/PRM-1 meter.

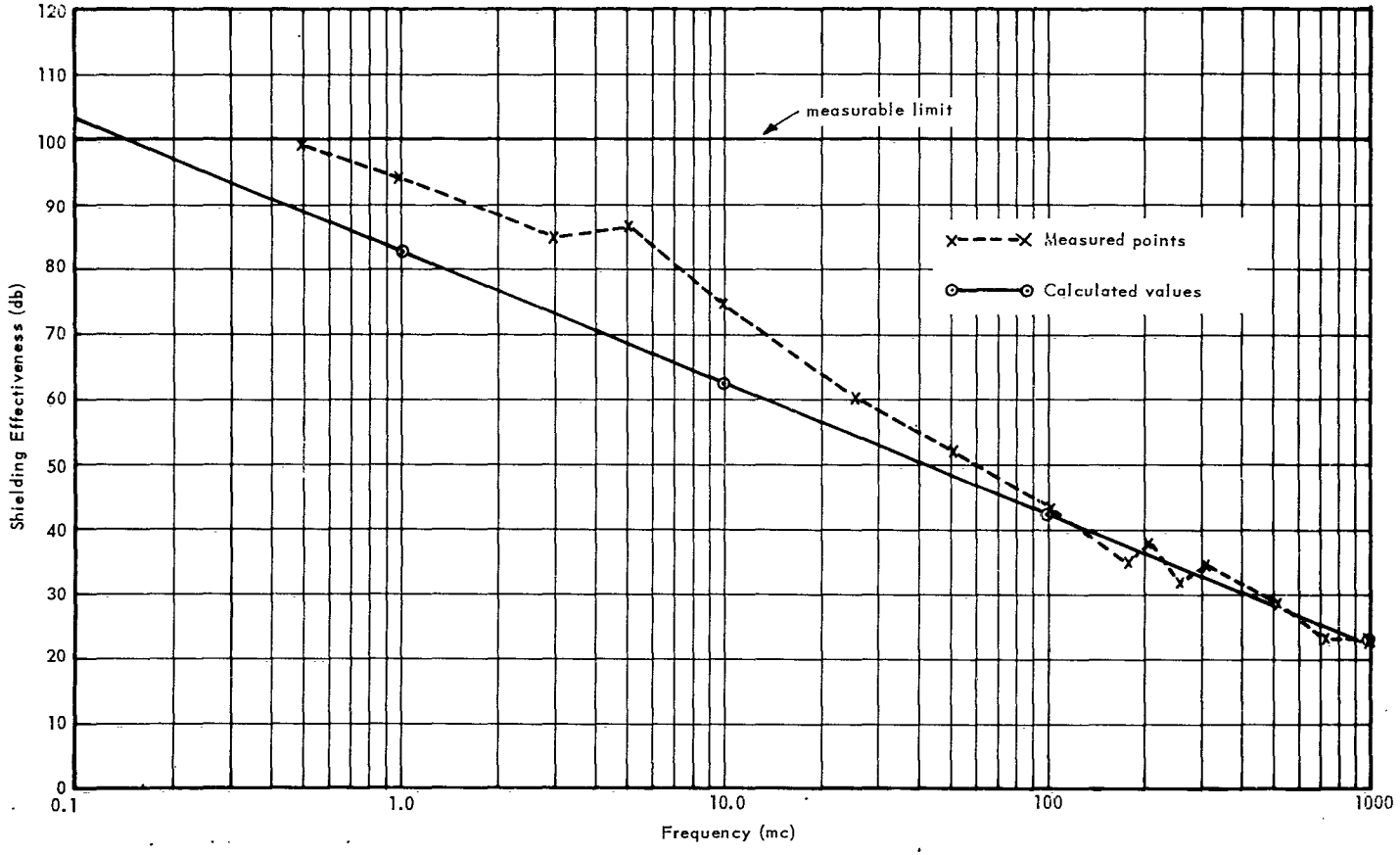

Figure 1. Values of shielding effectiveness of 10-ohm/square Type "A" conductive glass.

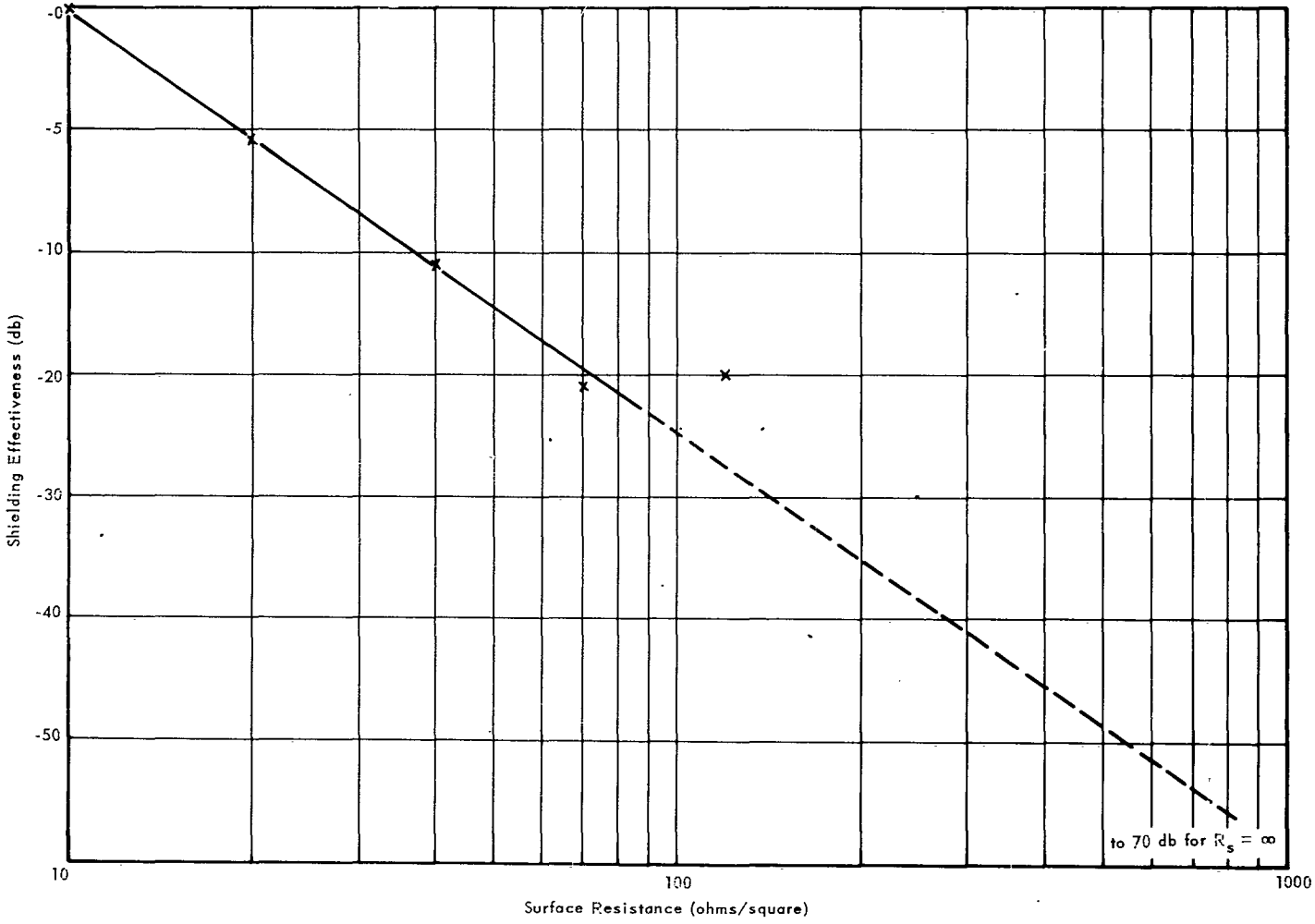

Figure 2. Reduction of shielding effectiveness versus surface resistance. Reference resistance is 10 ohms/square.

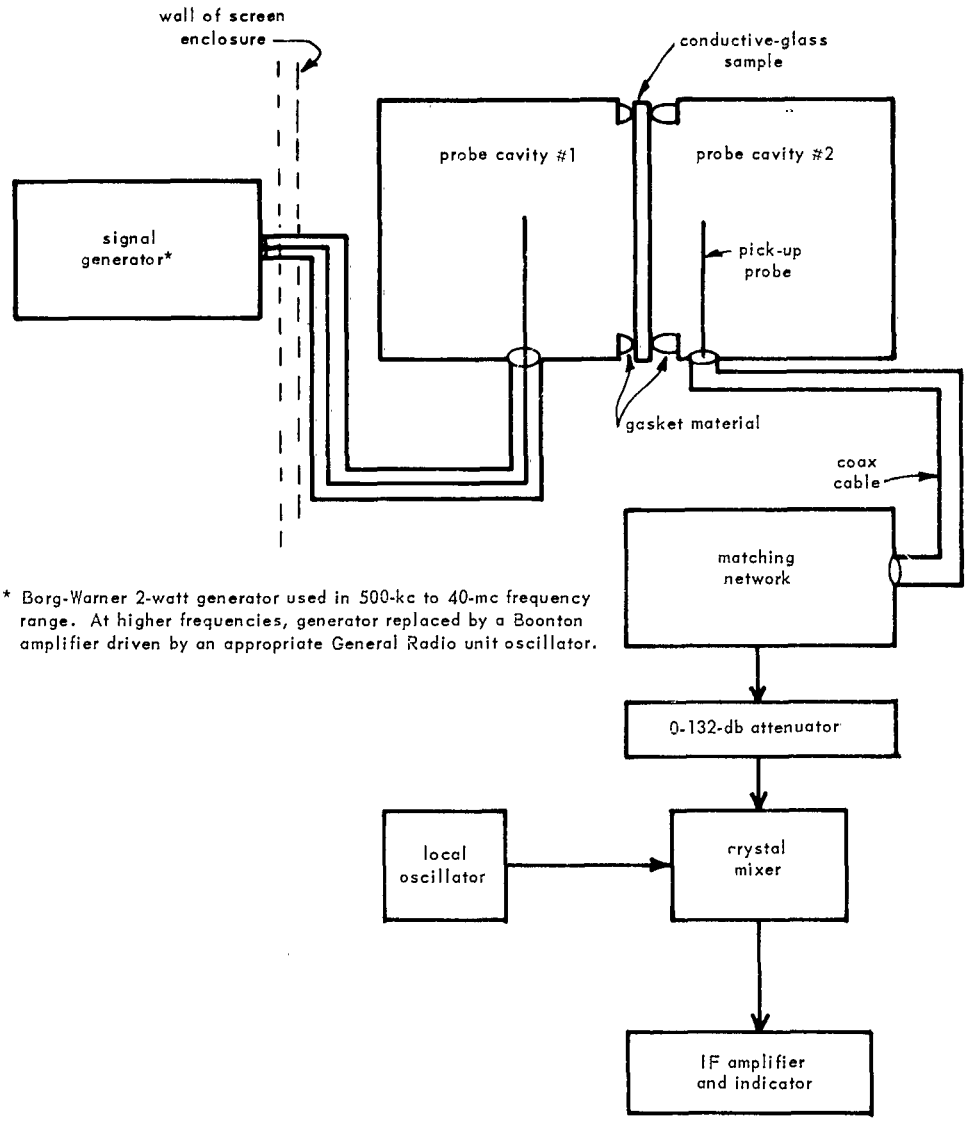

Figure 3. Block diagram of SE test setup.

Seven 4- by 4- by 1/4-inch conductive glass samples have been measured. Resistance values range from 9 to 125 ohms/square. In addition one sample with no coating at all ($R_s = \infty$) was tested. The SE versus frequency are presented graphically in Figures 4 through 6, inclusive. The data taken on all of the small samples is summarized in Table I.

The samples received were of two types of construction; diagrams are shown in Figures 7a and 7b. The SE of both the multiple-ply and single-ply configurations was determined, but in the frequency range under consideration the multiple-ply structure simply represented multiple layers of film in parallel. For example, 5 layers of 70-ohm/square material gave about the same SE as a single layer of 14-ohm/square material.

Samples tested are listed in Table II.

Table I. Decibel Values for SE of Conductive Glass

f (mc)	Surface Resistance (ohms/square)									
	∞	10	9	20	70	70[a]	40	40[b]	125	120
0.5	4	99	98	96	82	103	88	>103	88	79
1.0	6	94	99	94	80	104	87	>104	77	77
3.0	5	85	86	80	68	103	74	104	66	65
5.0	5	87	89	83	69	102	75	106	66	66
10.0	5	75	88	72	57	86	64	89	56	56
25.0	4	60	63	57	44	65	51	69	43	42
50.0	5	52	55	50	37	54	44	58	35	36
100.0	4	43	44	41	31	41	36	48	29	30
175.0	2	35	34	32	23	31	26	40	20	18
200.0	4	38	40	34	25	30	27	40	23	23
250.0	5	32	42	31	19	28	25	39	20	18
300.0	4	34	43	26	16	26	22	38	17	17
500.0	3	28	34	25	15	20	12	33	11	13
700.0	1	23	29	19	9	23	15	39	10	8
990.0	0	23	28	18	8	21	13	42	8	5
Type		A	C	A	A	A	A	A	B	A

[a] 3-ply
[b] 5-ply

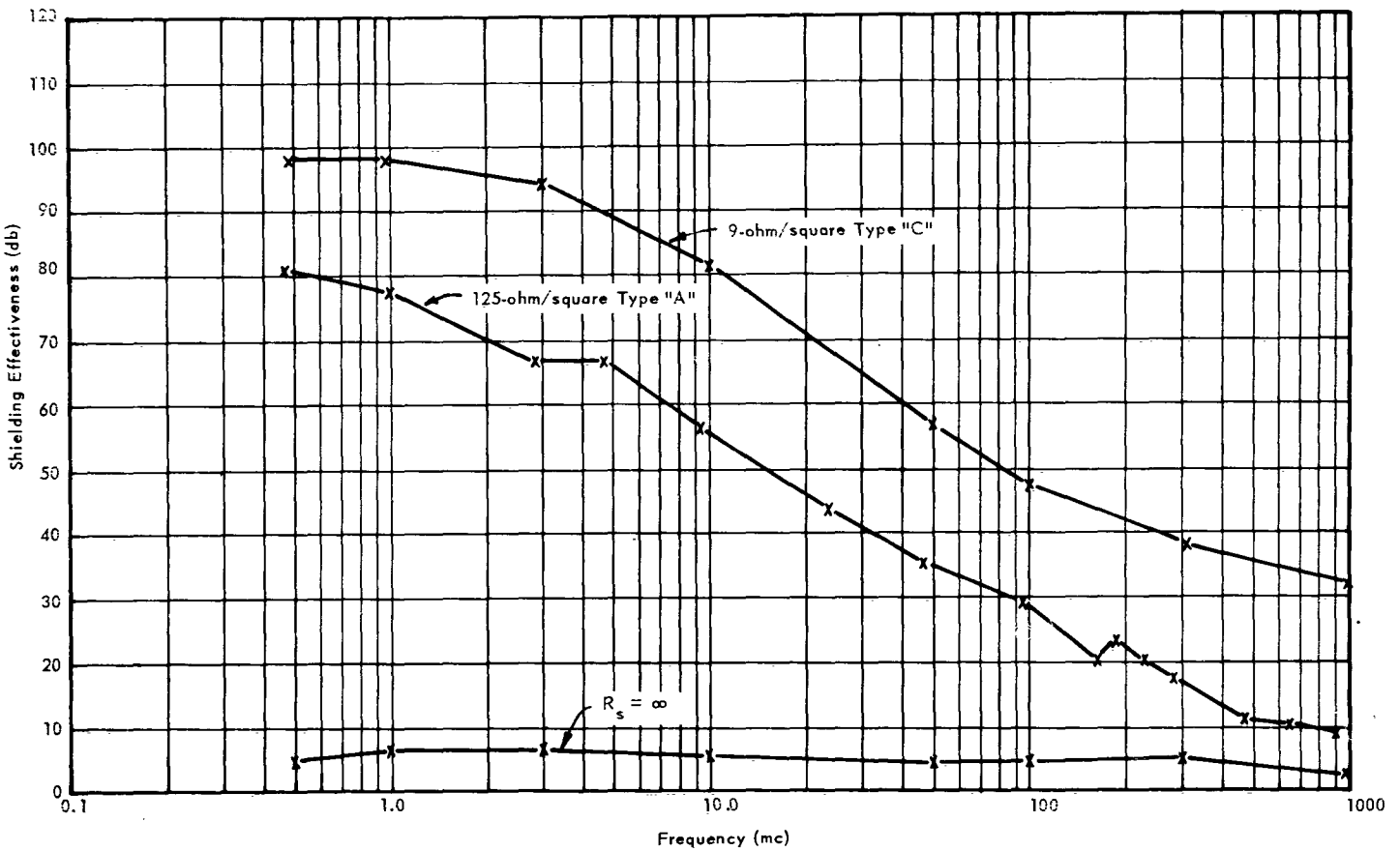

Figure 4. Measured values of shielding effectiveness for surface resistances of 9 ohms/square, 125 ohms/square, and $R_s = \infty$.

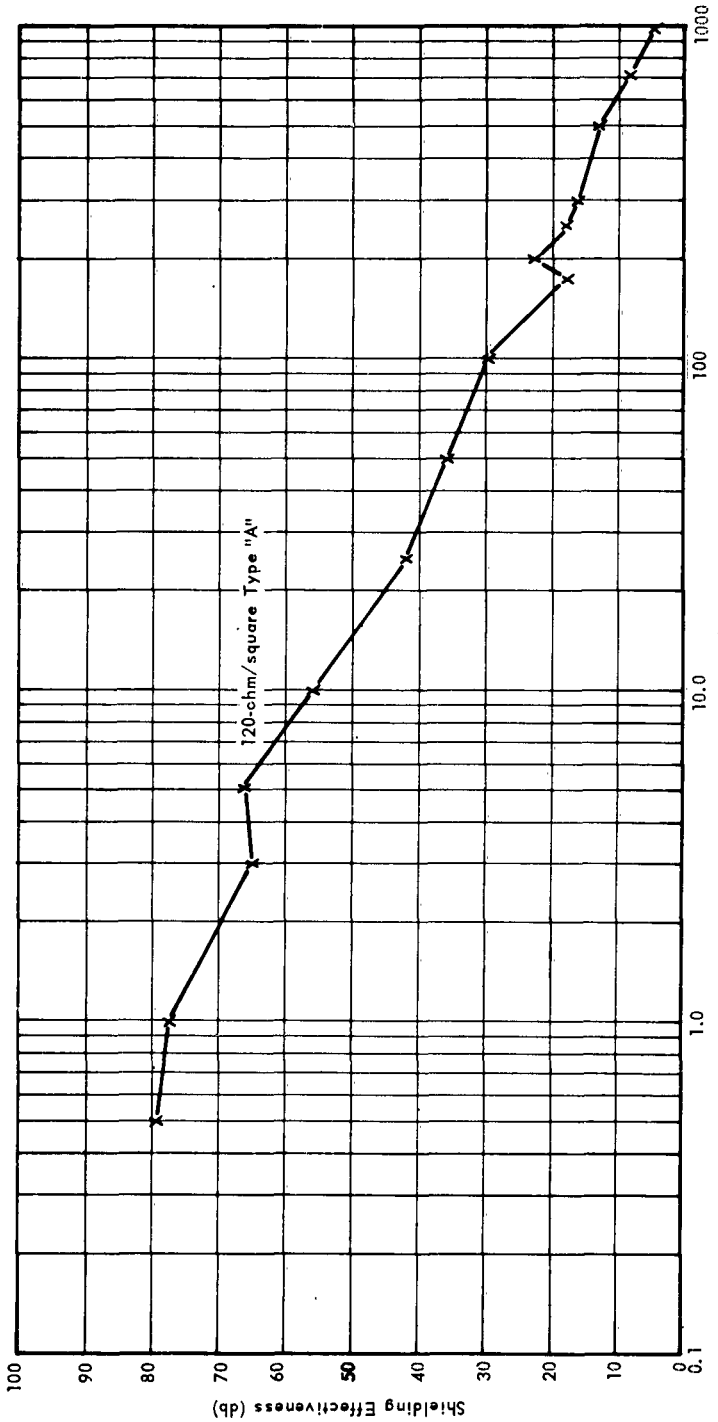

Figure 5. Shielding effectiveness for 120 ohms/square.

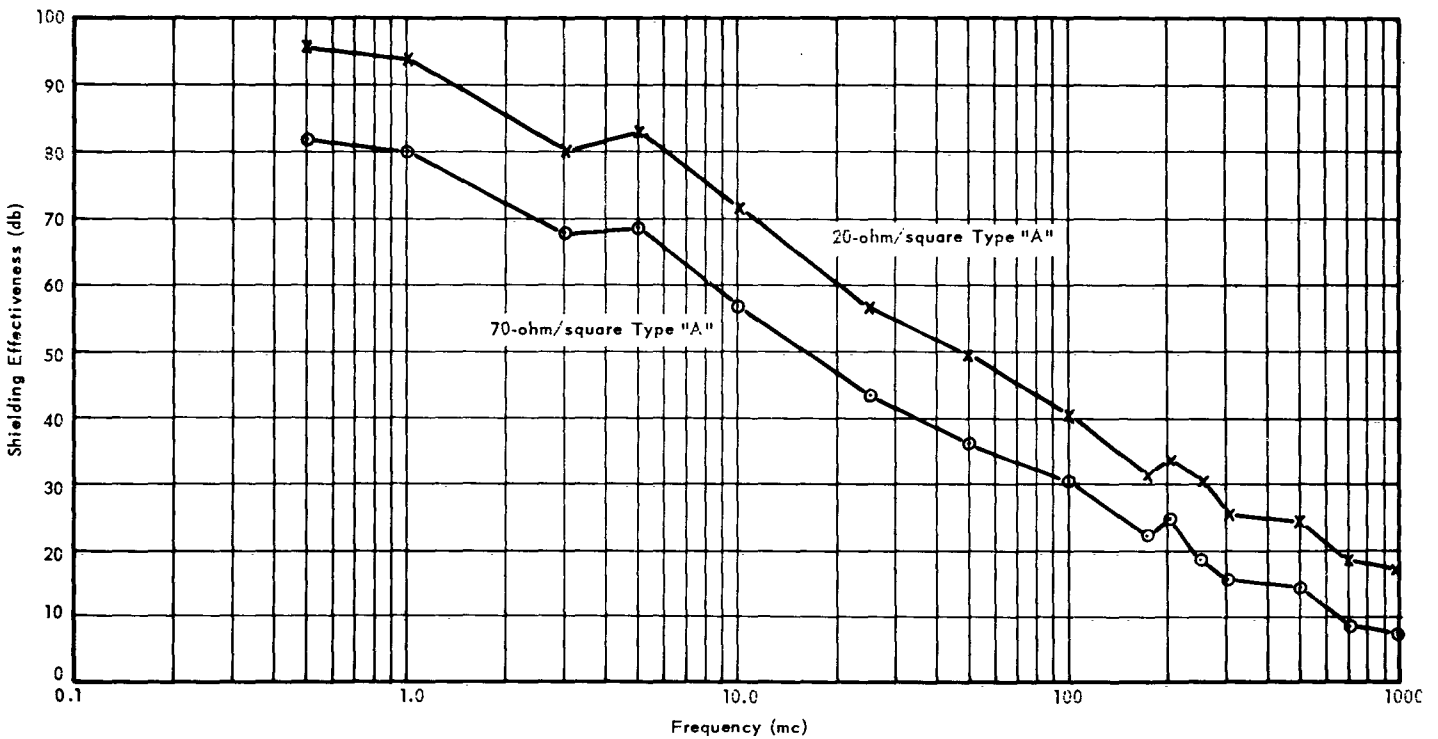

Figure 6. Shielding effectiveness of 70- and 20-ohm/square coated glass.

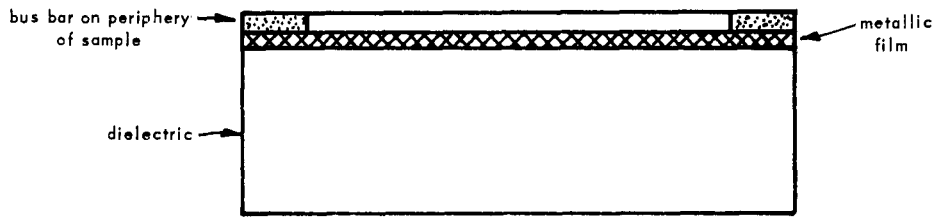

Figure 7a. Construction of single-ply samples.

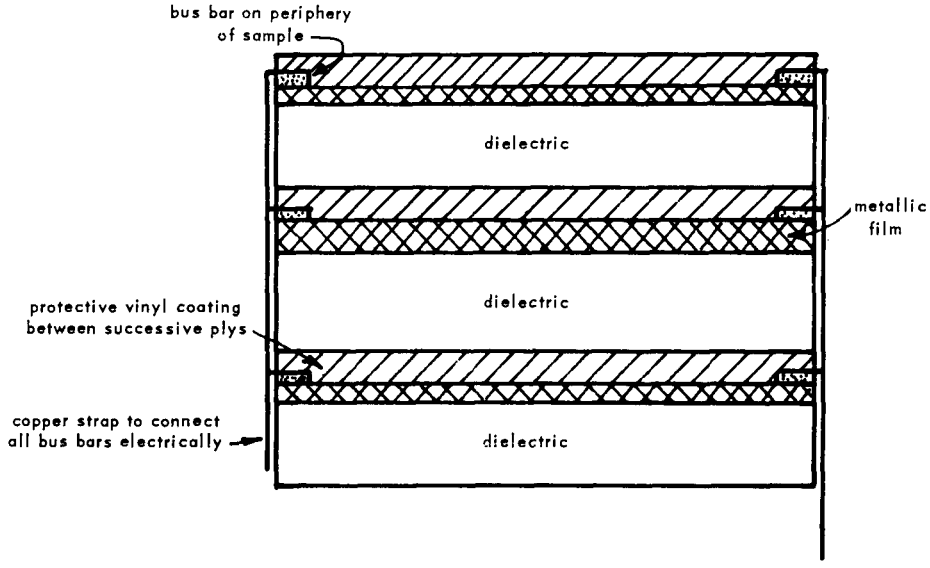

Figure 7b. Construction of multiple-ply samples.

Table II. Conductive Glass Tested

Type	Size	Resistance (ohms/square)	Number of Layers
A	4" x 4"	10	1
A	4" x 4"	20	1
A	4" x 4"	40	1
A	4" x 4"	70	1
A	4" x 4"	120	1
A	4" x 4"	70	3
A	4" x 4"	40	5
A	3' x 8'	10	1
B	4" x 4"	30	2 sides
B	4" x 4"	20	1
B	4" x 4"	125	1
C	4" x 4"	9	1
C	12" x 30"	9	1

EVALUATION OF LARGE SAMPLES

A different procedure was used in evaluating the large samples of conductive glass. These samples were installed in an existing portable screen room, which had been evaluated for its SE using the techniques set forth in Mil-E-4957A(ASG). See Figure 8.

The room was 10 by 10 by 8 feet with single-layer walls of 22-mesh copper screen. A portion of the screen wall was removed and replaced with a framework designed to hold the conductive glass. The framework also maintained electrical contact between the metallic film on the glass and the wall of the screen room. The SE of the room was determined, and the deterioration is indicated by the difference in the two curves given in Figure 9 for the 12- by 33-inch 9-ohm/square glass and in Figure 10 for the 8- by 3-foot 10-ohm/square glass.

Photographs of the samples mounted in the screen room are shown in Figures 11 and 12. The data for the 12- by 33-inch sample is given in Table III.

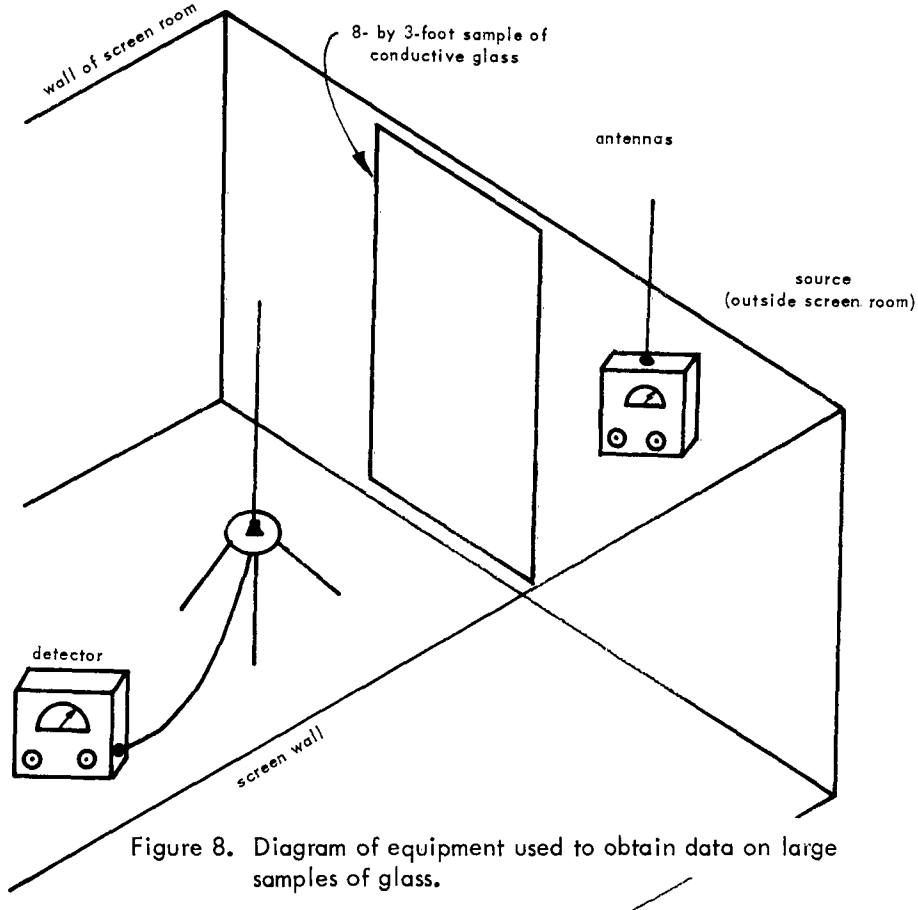

Figure 8. Diagram of equipment used to obtain data on large samples of glass.

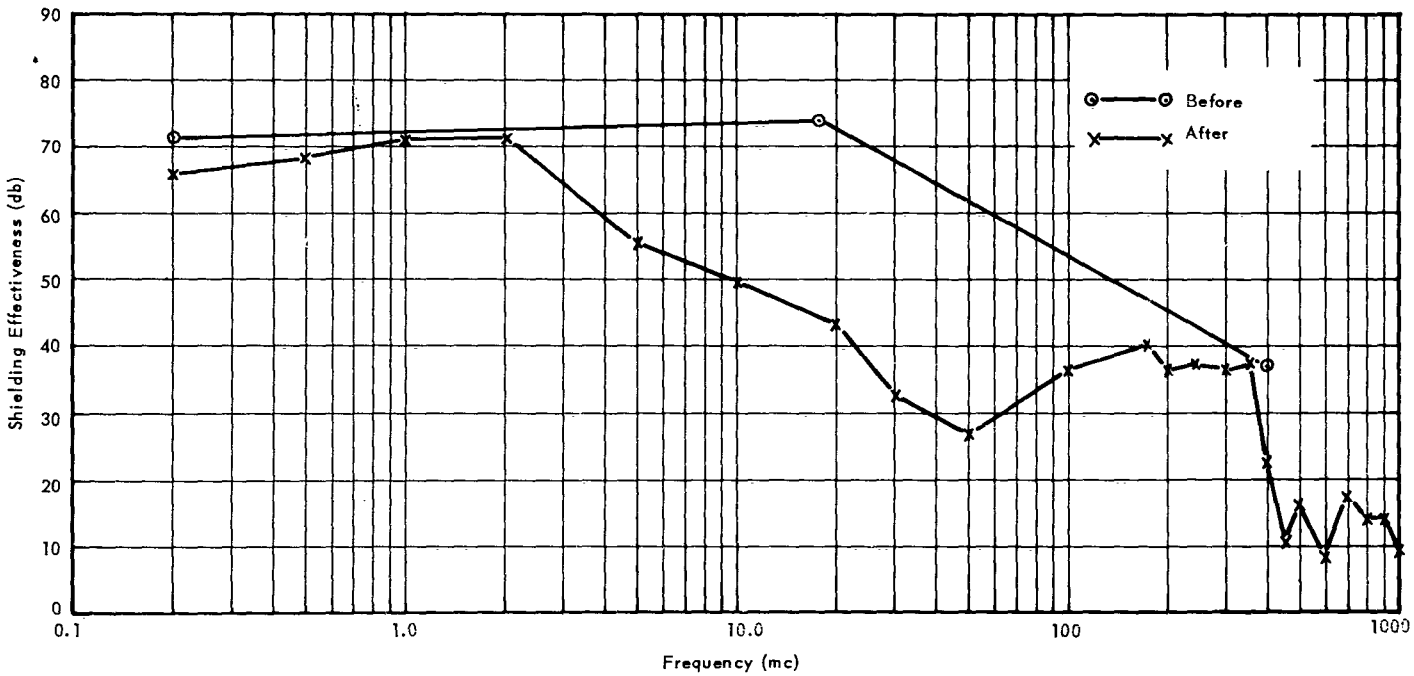

Figure 9. Shielding effectiveness of screen room before and after installing 12- by 33-inch sheet of 9-ohm/square glass.

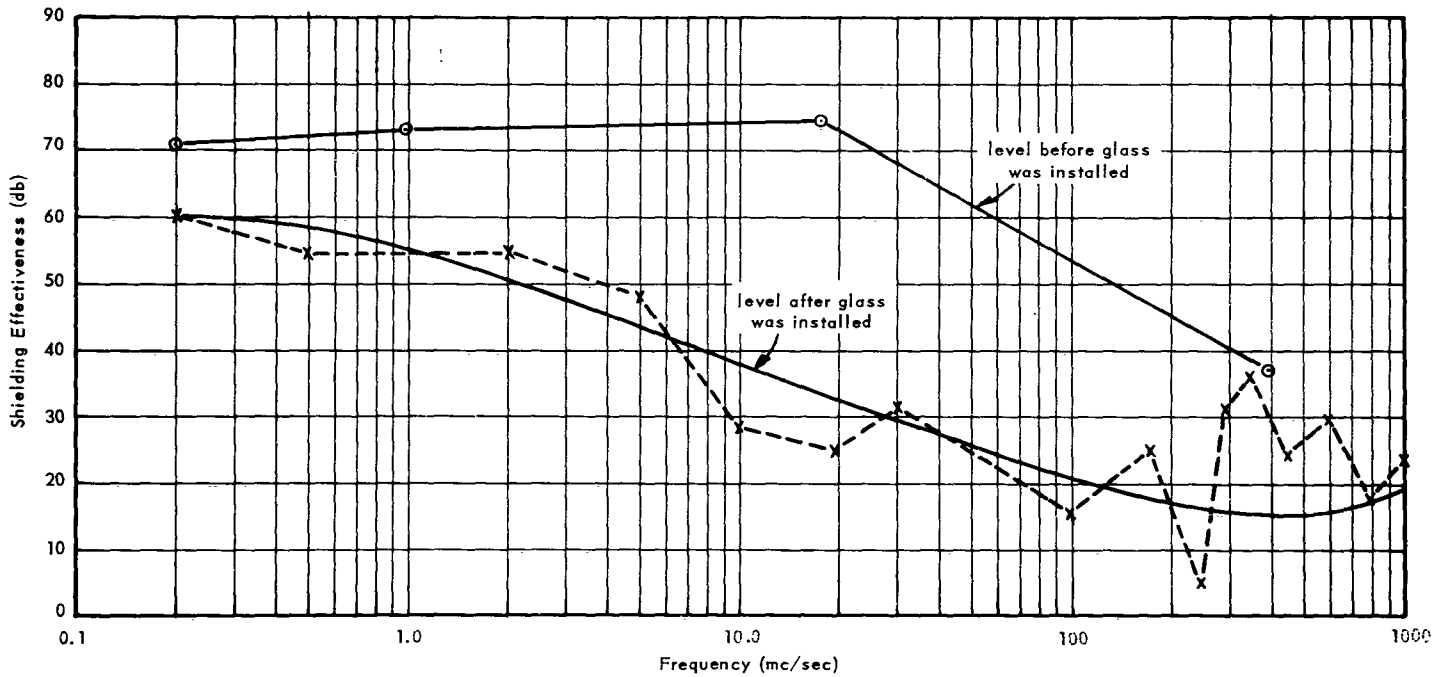

Figure 10. Shielding effectiveness of screen before and after installing 3- by 8-foot 9-ohm/square glass.

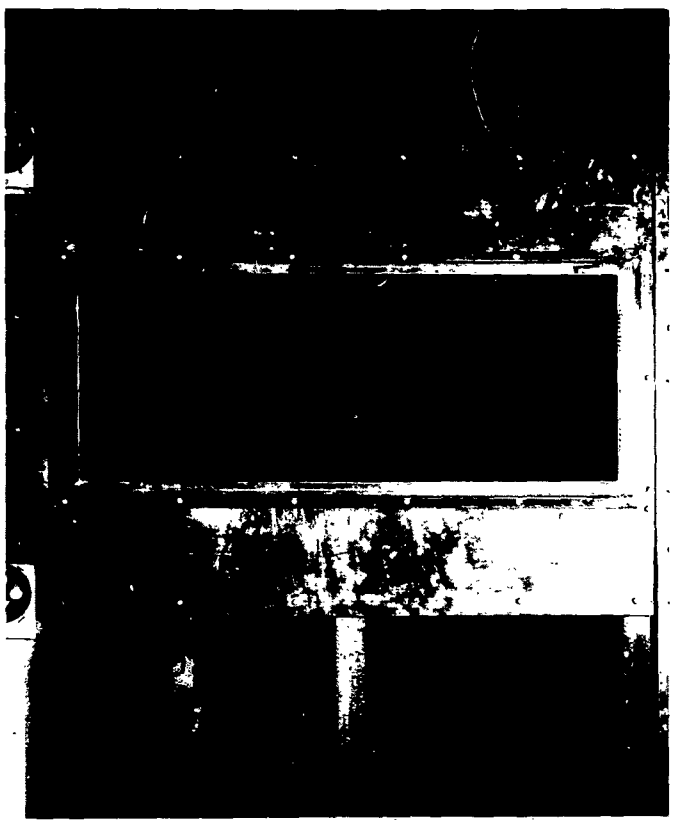

Figure 11. A 12- by 33-inch conductive-glass sheet mounted in wall of screen room.

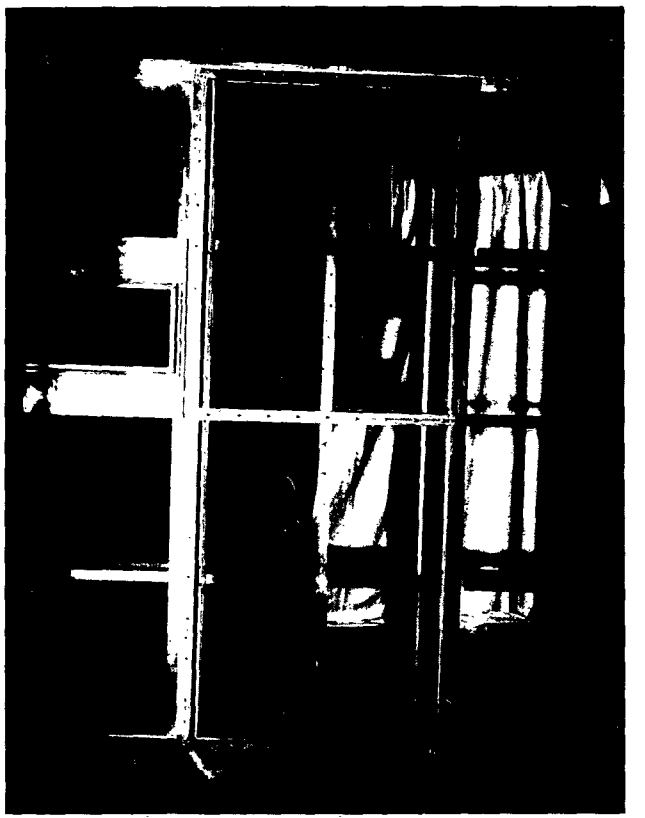

Figure 12. A 3- by 8-foot sheet of conductive glass installed in wall of screen room.

Table III. Peak Values for 12- by 33-Inch Sheet of 9-Ohm/Square Glass

f (mc)	P_1	P_2	P_1/P_2	20 log (P_1/P_2)
0.2	16,000	8.0	2,000.0	66.0
0.5	18,000	7.0	2,570.0	68.2
1.0	25,000	7.0	3,571.0	71.0
2.0	20,000	5.5	3,635.0	71.2
5.0	12,000	20.0	600.0	55.6
10.0	9,000	30.0	300.0	49.6
20.0	2,500	18.0	139.0	43.0
30.0	170	4.0	42.5	32.6
50.0	650	30.0	21.6	26.7
100.0	6,500	100.0	65.0	36.3
175.0	1,500	15.0	100.0	40.0
200.0	850	13.0	65.4	36.3
250.0	750	10.0	75.0	37.5
300.0	500	7.5	66.7	36.5
350.0	2,200	28.0	78.5	37.9
400.0	120	9.0	13.4	22.5
450.0	130	40.0	3.25	10.2
500.0	90	14.0	6.42	16.1
600.0	25	10.0	2.5	8.0
700.0	40	5.5	7.27	17.25
800.0	25	5.0	5.0	14.0
900.0	19	3.8	5.0	14.0
1,000.0	10	3.4	2.94	9.36

DETERMINATION OF MAGNETIC SHIELDING PROPERTIES

The magnetic shielding effectiveness of conductive glass is inherently poor due to the low permeability of the film. The loop on the AN/PRM-1 meter was oriented to maximize the measured H-vector component of the induced field. The edge of the loop was placed 1 inch away from the surface of the glass and was centered in the middle of the surface. Using a signal generator, and another loop oriented similarly as a source, the signal received from within the enclosure was recorded. Then another set of readings was taken with the loops the same distance apart and with similar orientation outside the enclosure. The ratio of these readings versus frequency is presented graphically in Figure 13.

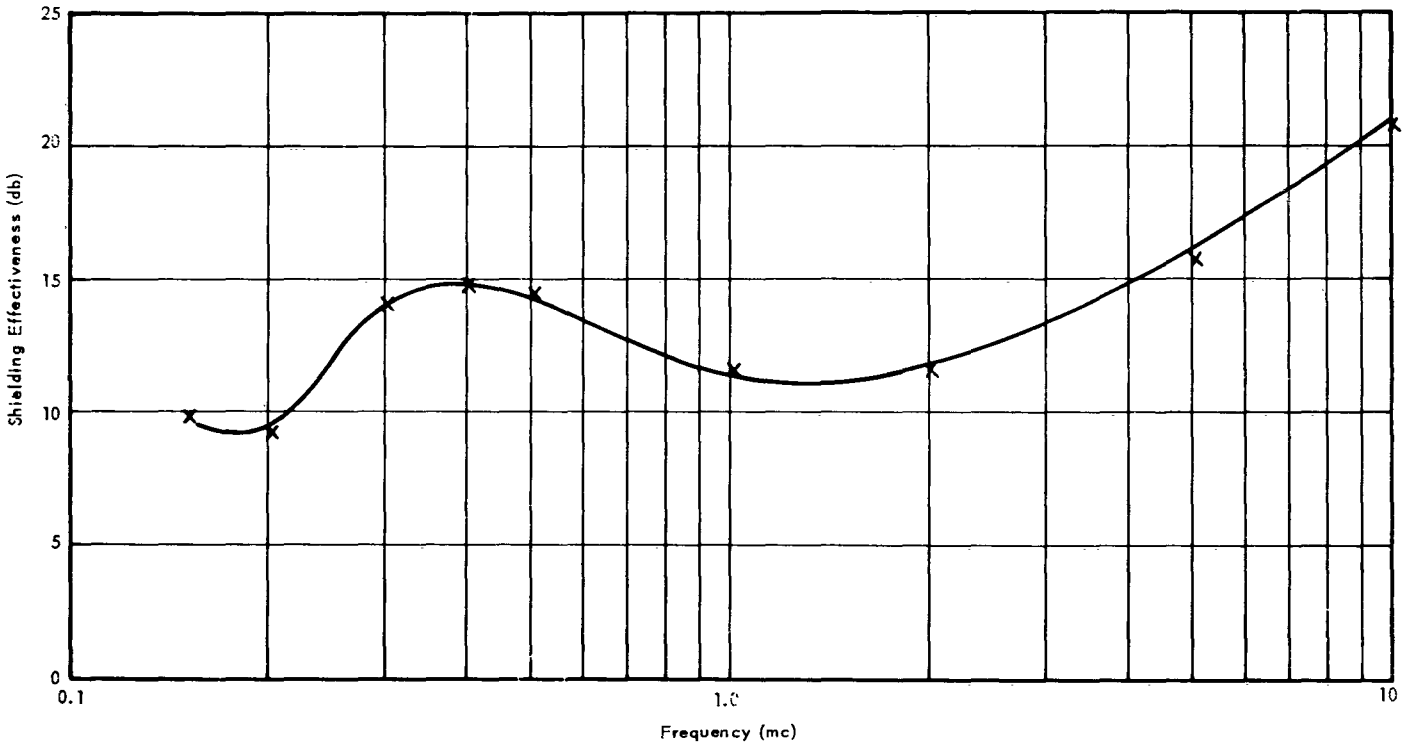

Figure 13. Low-impedance field measurements for 9-ohm/square Type "C" glass.

TRANSMISSION IN THE VISIBLE SPECTRUM FOR CONDUCTIVE GLASS

The transparency of the samples was determined using the setup shown in Figure 14. A tracing table was used for a light source so that a nearly uniform distribution of incident light was available at the surface of the sample.

The light-sensitive cell was moved to several positions along the surface of the sample and an average value of intensity was obtained. The sample was removed and the intensity at the same distance from the light source was determined. The ratio $I_1/I_2 \times 100$ expresses the average transmission as a percentage. The same procedure was followed for each of the single-ply samples. The values of the light transmission versus the resistivity of the surface are shown in Figure 15.

The light-transmission qualities of the 3- and 5-ply samples of type "A" material are not shown in Figure 14. These percentage values were:

40 ohms/square	5-ply	44.4%
70 ohms/square	3-ply	59.6%

CONCLUSIONS

1. The installation of single-ply conductive glass in an EMI-shielded room will provide shielding effectiveness in the range from 15 to 60 db, depending on the frequency under consideration.

2. At low frequencies the shielding effectiveness of conductive glass is related inversely to the value of the surface resistance. The transmission loss in the visible region increases with decreasing surface resistance. A compromise between light transmission and shielding integrity must be made.

3. In determining requirements for conductive glass in enclosure walls, due consideration for the nature of the incident wave front must be taken into account. In the near field, SE is a function not only of frequency but is strongly dependent on distrance from the surface to the source of radiation. When only far-field effects need be considered, the SE is determined by the wavelength of the radiation and the surface resistance of the glass.

4. Multiple-ply structures can be represented (at low frequencies) as equivalent single-ply configurations. For a given equivalent surface resistivity of the multiple-ply construction, the light-transmission loss is much greater than in a single-ply construction.

5. In general, films applied to the surface at room temperature are more fragile than those baked into the substratum.

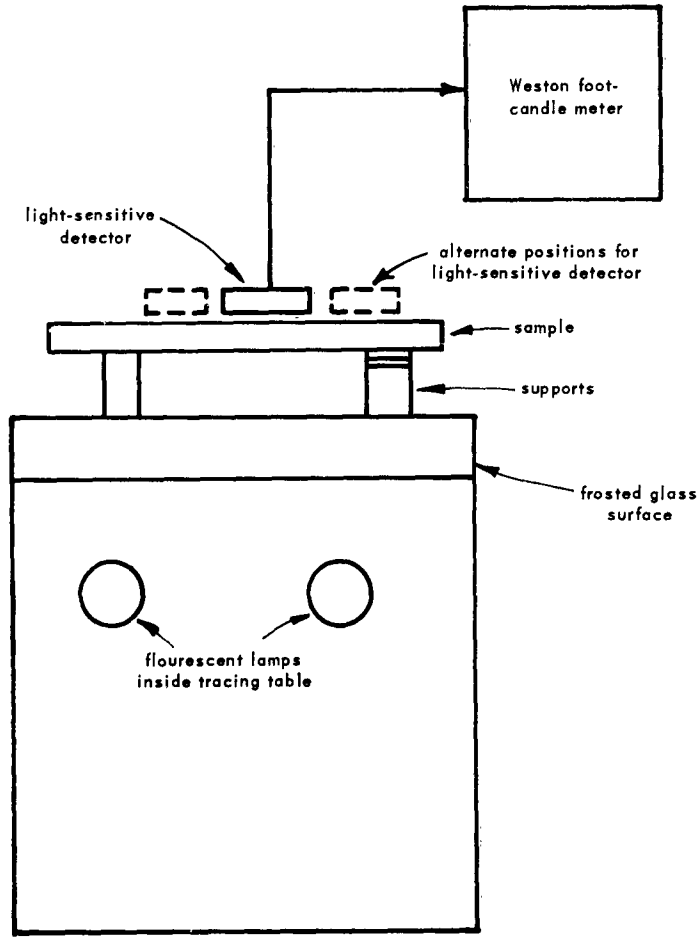

Figure 14. Test setup for determining light transmission.

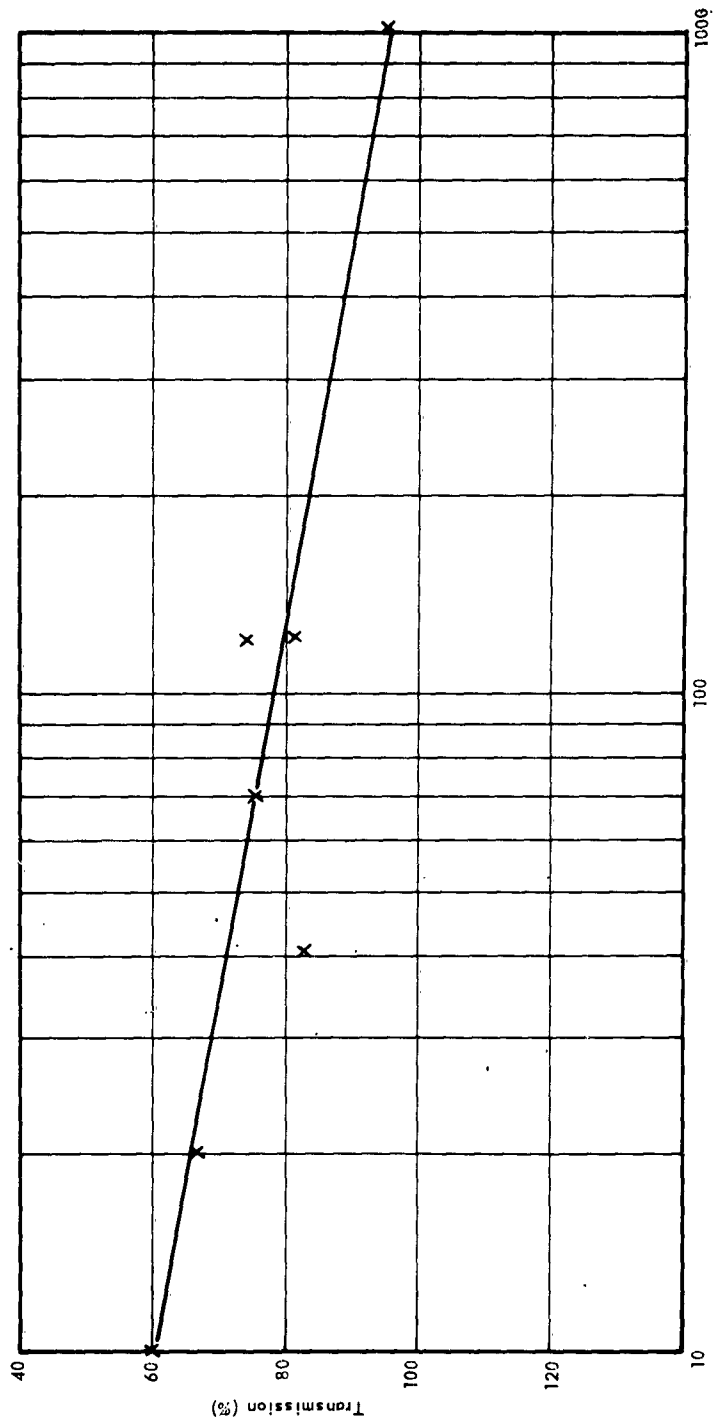

Figure 15. Light transmission versus surface resistance for transparent conductive glass.

RECOMMENDATIONS

1. The SE of conductive glass commercially available at this time has been investigated for both near- and far-field conditions[1] for a large variation in surface resistance, and no further evaluation effort is recommended.

2. Other methods of achieving acceptable light transmission which may offer acceptable values of SE and are worthy of investigation might include high-conductivity plasmas; conducting liquids confined to cells; new methods of applying films to glass; the use of materials in films that would achieve resistivities lower than 2 ohms/square yet give low light-transmission loss; conductive organic substances; and high-permeability materials that would give better magnetic shielding.

REFERENCES

1. Edward I. Hawthorne. "Electromagnetic Shielding with Transparent Coated Glass," Proceedings of IRE, Vol. 42, March 1954, pp. 548-553.

2. University of Pennsylvania, Moore School of Engineering. Investigation of the Shielding Properties of Conducting Glass by R. F. Schwartz, E. I. Hawthorne, and P. R. Adamson. Philadelphia, Pennsylvania, 26 September 1952, Interim Report for the period 26 June to 26 September 1952, Contract AF 30(602)-279.

3. Naval Research Laboratory. Report 4103, A Technique for Measuring the Effectiveness of Various Shielding Materials, by H. E. Dinger and J. E. Raudenbush. Washington, D. C., 22 January 1953.

4. S. A. Schelkunoff. Electromagnetic Waves. D. Van Nostrand Co., Inc., New York, 1943. p. 81.

5. J. D. Krause. Electromagnetics. McGraw-Hill Book Company, Inc., New York, 1953. p. 499.

6. J. A. Stratton. Electromagnetic Theory, first edition. McGraw-Hill Book Company, Inc., New York, 1941. p. 283.

7. U. S. Naval Air Development Center. Report No. NADC-EL-N5507, Problems in Shielding Electrical and Electronic Equipments, by C. S. Vasaka. Johnsville, Pennsylvania, 8 June 1955.

8. K. Fuchs and H. H. Wills. "The Conductivity of Thin Metallic Films According to the Electron Theory of Metals," Cambridge Philosophical Society Proceedings, Vol. 34. Bristol, England, 1938. pp. 100-108.

DEFINITION OF TERMS

A = shielding effectiveness due to absorption

B = correction factor used when $A < 10$ db

BL = reflection loss due to one or more boundaries

BL_i = reflection loss due to the i^{th} boundary

c = velocity of wave propagation

E = electric field intensity at any point (volts/meter)

E_o = initial value of the electric field (volts/meter)

E^i = incident component of electric vector (volts/meter)

E^R = reflected component of electric vector (volts/meter)

E_1 = voltage measured when the sample is not in the cavity (volts)

E_2 = voltage measured when the sample is in the cavity (volts)

f = frequency (cps)

H^i = incident magnetic component (amps/meter)

H^r = reflected magnetic component (amps/meter)

H^* = complex conjugate of H

I_o = initial value of currect distribution on dipole

I_1 = initial intensity (foot candles)

I_2 = final intensity (foot candles)

$j = \sqrt{-1}$

$k = \epsilon_g / \epsilon_o$ = dielectric constant for glass

L = length of dipole (meters)

R = sample resistance (ohms)

r = separation between source and surface (meters)

R_s = surface resistance (ohms/square)

$\vec{S}$ = Poynting vector

SE_{total} = (A + BL, A > 10 db)/(B + BL, A < 10 db)

t = film thickness (meters)

w = width of sample (arbitrary units)

z_f = impedance of wave in film (ohms)

z_g = impedance of wave in glass (ohms)

z_w = impedance of wave in near field (ohms)

α = attenuation constant (nepers/meter)

β = $2\pi/\lambda$ (radians/meter)

γi = propagation constant through the i^{th} medium = $\alpha + j\beta$

Δ = length of sample (arbitrary units)

δ = μ_o/ϵ_o = impedance of free space (ohms)

ϵ_g = permittivity of glass

ϵ_o = $(1/36\pi) \times 10^{-9} = 8.854 \times 10^{-12}$ farads/meter (permittivity of free space)

λ = wavelength (meters)

μ_o = $4\pi \times 10^{-7} = 1.257 \times 10^{-6}$ henrys/meter (permeability of free space)

σ_g = conductivity of glass (mho/meter)

τ = time (seconds)

ω = $2\pi f$

Appendix A

MATHEMATICAL DEVELOPMENT OF THE EXPRESSIONS FOR SHIELDING EFFECTIVENESS

Shielding effectiveness can be defined as the reduction in level of an EM wave at a point in space after a conductive barrier has been inserted bewteen that point and the source. The level is reduced by absorption in passing through the barrier and by reflection from its boundaries. For thin films the dominant effect is that of reflection. The reflection is governed primarily by the impedance of the incident wave and the impedance of the surface.

The attenuation due to reflection from each of the surfaces encountered can be determined from the boundary equations that must be satisfied by the wave. A pictorial representation of the film-glass combination under consideration is shown in Figure 16. In addition, the boundary values are given in Equations 1 to 15.

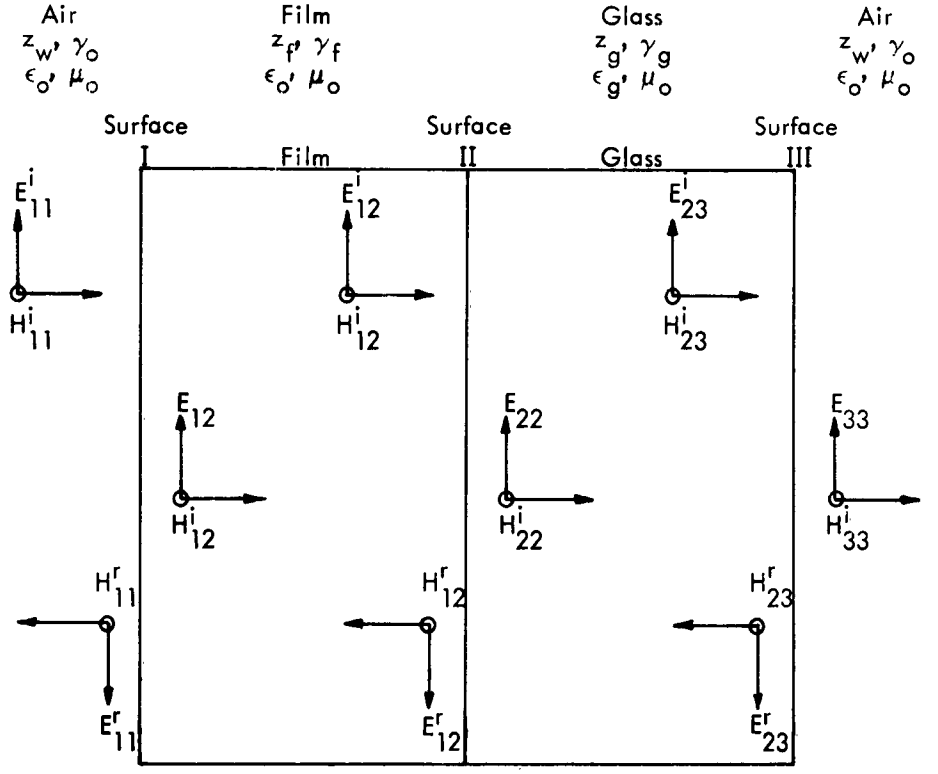

Figure 16. Vector diagrams for incident and reflected wave components.

Surface I	Surface II	Surface III
(1) $E^i_{11} + E^r_{11} = E_{12}$	(6) $E^i_{12} + E^r_{12} = E_{22}$	(11) $E^i_{23} + E^r_{23} = E_{33}$
(2) $H^i_{11} + H^r_{11} = H_{12}$	(7) $H^i_{12} + H^r_{12} = H_{22}$	(12) $H^i_{23} + H^r_{23} = E_{33}$
(3) $H^i_{11} = \frac{E^i_{11}}{z_w}$	(8) $H^i_{12} = \frac{E^i_{12}}{z_f}$	(13) $H^i_{23} = \frac{E^i_{23}}{z_g}$
(4) $H^r_{11} = \frac{-E^r_{11}}{z_w}$	(9) $H^r_{12} = \frac{-E^r_{12}}{z_f}$	(14) $H^r_{23} = \frac{-E^r_{23}}{z_g}$
(5) $H_{12} = \frac{E_{12}}{z_f}$	(10) $H_{22} = \frac{E_{22}}{z_g}$	(15) $H_{33} = \frac{E_{33}}{z_w}$

The boundary loss (BL_1) at surface I is developed by introducing Equations 3, 4, and 5 into 2, obtaining the following:

$$\frac{E^i_{11}}{z_w} - \frac{E^r_{11}}{z_w} = \frac{E_{12}}{z_f} \tag{16}$$

From Equations 1 and 16, E^r_{11} can be eliminated, and the ratio

$$\frac{E_{12}}{E^i_{11}} = \frac{2z_f}{z_w + z_f} \tag{17}$$

can be established. This ratio can be further expressed as the boundary loss,

$$BL_1 = -20 \log_{10} \frac{2|z_f|}{|z_w + z_f|} \tag{18}$$

In a similar manner the boundary-loss expressions for the successive surfaces may be developed. Substituting Equations 8, 9, and 10 into 7 and using the new expression in conjunction with 6 the boundary loss at surface II can be written as

$$BL_2 = -20 \log_{10} \frac{2|z_g|}{|z_g + z_f|} \tag{19}$$

Also,

$$BL_3 = -20 \log_{10} \frac{2|z_w|}{|z_g + z_w|} \tag{20}$$

is the boundary loss for surface III.

The total boundary loss can be written as

$$BL = BL_1 + BL_2 + BL_3 = 20 \log_{10} \frac{|z_w + z_f||z_g + z_f||z_g + z_w|}{8|z_f||z_g||z_w|} \tag{21}$$

The intrinsic impedance of the film z_f can be written as[4]

$$z_f = (1 + j)\sqrt{\frac{\mu_o \omega}{2\sigma_f}} \tag{22}$$

and

$$|z_f| = \sqrt{\frac{\mu_o \omega}{\sigma_f}} \tag{23}$$

The intrinsic impedance of the glass is developed as follows[4]

$$z_g = \sqrt{\frac{\mu_o}{\epsilon - j\frac{\sigma_g}{\omega}}} = \sqrt{\frac{\omega\mu_o}{\omega\epsilon - j\sigma_g}} \tag{24}$$

The term $\omega\epsilon$ ranges from $\cong 3 \times 10^{-4}$ to $\cong 0.3$ over the frequency range of 1 to 1,000 mc; whereas the conductivity of glass is on the order of 10^{-12} mho/meter. Therefore $\omega\epsilon >> \sigma_g$. Thus Equation 24 becomes

$$z_g \cong \sqrt{\frac{\mu_o}{\epsilon_g}}$$

but

$$\frac{\epsilon_g}{\epsilon_o} \equiv k$$

so that

$$z_g = \frac{\delta_o}{\sqrt{k}} \tag{25}$$

where

$$\delta_o = \sqrt{\frac{\mu_o}{\epsilon_o}}$$

Now consider the impedance of the incident wave, z_w, with particular emphasis on the near-field condition; i.e., the source is close to the surface of interest. It has been shown[5] that the field equations for a short dipole ($L << \lambda$) are

$$E_r = \frac{\nu \cos\theta}{2\pi\epsilon_o}\left(\frac{1}{cr^2} + \frac{1}{j\omega r^3}\right) \tag{26}$$

$$E_\theta = \frac{\nu \sin\theta}{4\pi\epsilon_o}\left(\frac{j\omega}{c^2 r} + \frac{1}{cr^2} + \frac{1}{j\omega r^3}\right) \tag{27}$$

$$H_\varphi = \frac{\nu \sin\theta}{4\pi}\left(\frac{1}{r^2} + \frac{j\omega}{cr}\right) \tag{28}$$

$$H_\theta = H_r = E_\varphi = 0$$

where $$\nu = I_o L e^{j(\omega t - \beta r)}$$

These components of the field vectors $\vec{E}$ and $\vec{H}$ are shown in Figure 17, along with their relationship to the location of the dipole in the polar coordinate system. It is profitable to examine the Poynting Vector $\vec{S}$ to determine the direction in which energy is propagated from the short dipole under near-field conditions.[6] $\vec{S}$ is defined as

$$\vec{S} = \vec{E} \times \vec{H}^*$$

$$\vec{S} = \begin{vmatrix} \hat{r} & \hat{\theta} & \hat{\varphi} \\ E_r & E_\theta & 0 \\ 0 & 0 & H^*_\varphi \end{vmatrix} = \hat{r} E_\theta H^*_\varphi - \hat{\theta} E_r H^*_\varphi$$

which becomes

$$S = \frac{\nu^2 \sin^2\theta}{16\pi^2\epsilon_o}\left(\frac{\omega}{c^3 r^2} + \frac{1}{j\omega r^5}\right)\hat{r} - \frac{\nu^2 \sin\theta\cos\theta}{8\pi^2\epsilon_o}\left(-\frac{j\omega}{c^2 r^3} + \frac{1}{j\omega r^5}\right)\hat{\theta} \tag{29}$$

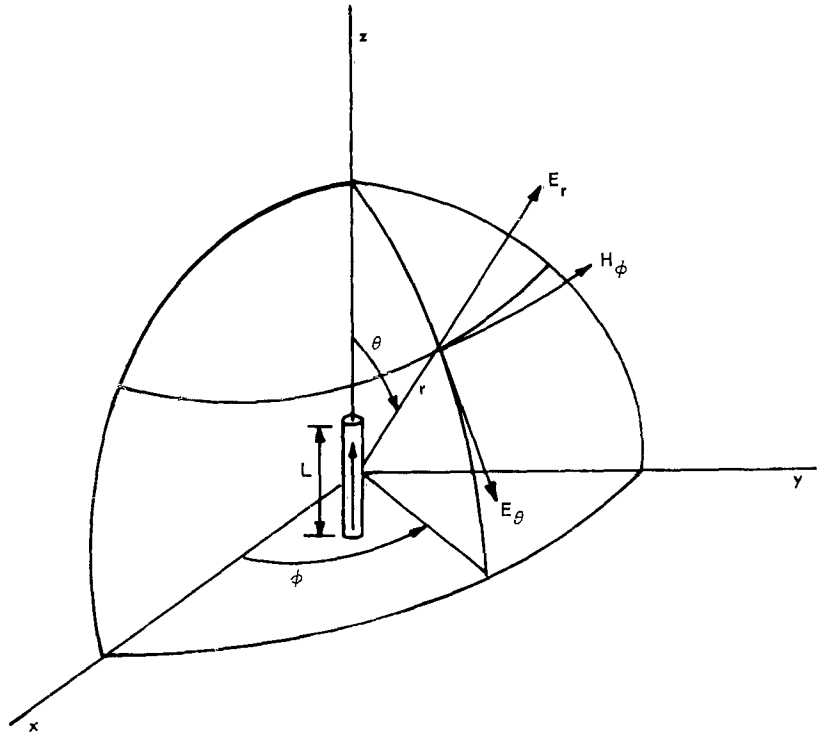

Figure 17. Coordinate system indicating components E_θ, E_r, H_φ and location of short dipole.

The term indicating energy flow in the $\hat{\theta}$ direction as well as one term in r direction are imaginary and represent energy stored in the field and not radiated. Propagation occurs in the $\hat{r}$ direction as indicated by the real component of $\vec{S}$ in that direction. The impedance of the radiated wave is

$$z_w = \frac{E_\theta}{H_\varphi} = \frac{1}{\epsilon_o c r \omega}\left(\frac{r^3\omega^3 - jc^3}{c^2 + r^2\omega^2}\right) \tag{30}$$

Under the stipulation of near-field conditions where $r << \lambda$, then

$$z_w = \frac{-j}{\epsilon_o r \omega} \tag{31}$$

The impedance of the wave may now be used to help evaluate Equation 21. The absolute values $|z_w + z_f|$, $|z_g + z_f|$, and $|z_g + z_w|$ can be written as

$$|z_w + z_f| = \left[\frac{\mu_o\omega}{\sigma_f} + \frac{1}{(\epsilon_o\omega r)^2} - \frac{2}{\epsilon_o\omega r}\sqrt{\frac{\mu_o\omega}{2\sigma_f}}\right]^{1/2} \tag{32}$$

$$|z_g + z_f| = \left(\frac{\mu_o\omega}{\sigma_f} + \frac{\delta_o^2}{k} + 2\delta_o\sqrt{\frac{\mu_o\omega}{2\sigma_f k}}\right)^{1/2} \tag{33}$$

$$|z_g + z_w| = \left[\frac{\delta_o^2}{k} + \frac{1}{(\epsilon_o\omega r)^2}\right]^{1/2} \tag{34}$$

Certain simplifications of Equations 32, 33, and 34 are in order when ω is small, $r \approx 2.5$ cm and $\sigma_f = 10^5$ mho/meter (see Appendix B). These conditions represent the experimental values discussed. The dominant term in Equations 32 and 34 is $1/(\epsilon_o \omega r)^2$, and, in Equation 33, δ_o^2/k takes precedence. Under these circumstances Equation 21 can be written as

$$BL = 20 \log_{10} \frac{1}{8\epsilon_o \omega r \sqrt{\frac{\mu_o \omega}{\sigma_f}}} \tag{35}$$

It is interesting to note that parameters describing the glass itself have now vanished and the BL is due only to parameters of the film. Equation 35 is essentially the equation developed by C. S. Vasaka[7] and to a certain extent that developed by H. E. Dinger and J. E. Raudenbush[3] for the reflection from a metallic sheet.

Absorption contributes to SE by reducing the wave intensity in passing through the material in question. Assume that the film is homogeneous so that γ_f, the propagation constant, does not vary as a function of the thickness t. Also assume a wave function of the form

$$E = E_o \exp j(\omega\tau - \gamma_f t) \tag{36}$$

$$\gamma_f = \omega \sqrt{\mu \left(\epsilon - j\frac{\sigma_f}{\omega}\right)} \qquad \text{(see Reference 6)}$$

$$\gamma_f = \sqrt{\mu\omega}\left(\omega^2\epsilon^2 + \sigma_f^2\right)^{1/4} (\cos\varphi + j \sin\varphi) \tag{37}$$

$$\varphi = 1/2 \tan^{-1}\left(\frac{-\sigma_f}{\omega\epsilon}\right) \tag{38}$$

Substituting Equations 37 and 38 into 36, and presenting the time-maximized real portion of E, gives

$$\mathrm{Re}(E)_{max} = E_o \exp\left\{- t\sqrt{\mu\omega}\left(\omega^2\epsilon^2 + \sigma^2\right)^{1/4} \sin\left[\frac{\tan^{-1}}{2}\left(\frac{\sigma_f}{\omega\epsilon}\right)\right]\right\} \quad (39)$$

where $$\cos\left[\omega\tau - t\sqrt{\mu\omega}\left(\epsilon^2\omega^2 + \sigma_f^2\right)^{1/4} \cos\varphi\right]_{max} = 1 \quad (40)$$

The absorption in passing through a material of thickness t with properties μ, σ, ϵ and at frequency $f = \omega/2\pi$ is

$$A = -20 \log_{10} \frac{\mathrm{Re}(E)_{max}}{E_o} \quad (41)$$

Equation 39 can be simplified by considering the following for the film:

$$\sigma_f >> \omega\epsilon$$

so that $$\frac{\tan^{-1}}{2}\left(\frac{\sigma_f}{\omega\epsilon}\right) \rightarrow \frac{\pi}{4}$$

and $$\sin\left[\frac{\tan^{-1}}{2}\left(\frac{\sigma_f}{\omega\epsilon}\right)\right] \rightarrow \frac{\sqrt{2}}{2}$$

Also $$\left(\omega^2\epsilon^2 + \sigma_f^2\right)^{1/4} \rightarrow \sqrt{\sigma_f}$$

so that $$A = 20 \times 0.43429\, t\sqrt{\frac{\mu\omega\sigma_f}{2}} \quad (42)$$

A typical numerical value for the absorption term A can be determined where

$$t \cong 10^{-6} \text{ meters}$$

$$\mu = \mu_o = 1.25 \times 10^{-6} \text{ h/meter}$$

$$\sigma_f = 10^5 \text{ mho/meter}$$

$$\omega = 6.28 \times 10^6$$

Then $A \cong 5.44 \times 10^{-3}$ db at a frequency of 1 mc; A increases slowly with increasing frequency, in fact with $\sqrt{\omega}$. Thus it appears that the absorption term A for the thin film can be neglected.

Before the absorption term can be totally ignored, however, a correction factor must be added to BL because A is small. For "electrically thin" materials,[7] or $A < 10$ db, the correction factor is

$$B = 20 \log_{10} \left| 1 - \left(\frac{z_f - z_w}{z_f + z_w} \right)^2 10^{-\frac{A}{10}} (\cos\theta - j \sin\theta) \right| \qquad (43)$$

where $$\theta = 3.59\, t \sqrt{f \mu \sigma_f}$$

The impedance of the wave z_w is much greater than the impedance of the film z_f over the frequency range under consideration so that

$$\left(\frac{z_f - z_w}{z_f + z_w}\right)^2 = \left(\frac{1 - \frac{z_w}{z_f}}{1 + \frac{z_w}{z_f}}\right)^2 \cong 1$$

and the angle θ is much less than 10 degrees over the same frequency range so that

$$\cos\theta \cong 1 \text{ and } \sin\theta \cong \theta$$

Also the factor $10^{-\frac{A}{10}} \approx 1$ for small values of A. Thus Equation 43 can be written as

$$B = 20\log_{10}\theta = 20\log_{10}(3.59\, t\sqrt{f\mu\sigma_f}) \tag{44}$$

This can be combined with Equation 35 to become

$$SE_{total} = BL + B = 20\log_{10}\frac{3.59\, t\sqrt{f\mu\sigma_f}}{8\epsilon_o\omega r\sqrt{\frac{\mu\omega}{\sigma_f}}} = 20\log_{10}\left(\frac{3.59\, t\sigma_f}{8\epsilon_o(2\pi)^{3/2}fr}\right) \tag{45}$$

The surface resistance of the film (from Appendix B) is

$$R_s = \frac{1}{t\sigma_f}$$

Thus Equation 45 becomes

$$SE_{total} = 190.12 - 20\log_{10}(frR_s) \tag{46}$$

This equation has been compared with experimental data taken on a sample with an R_s of 10 ohms/square and a separation between radiator and surface of r = 1 inch. Both the experimental curve and Equation 46 are shown in Figure 1.

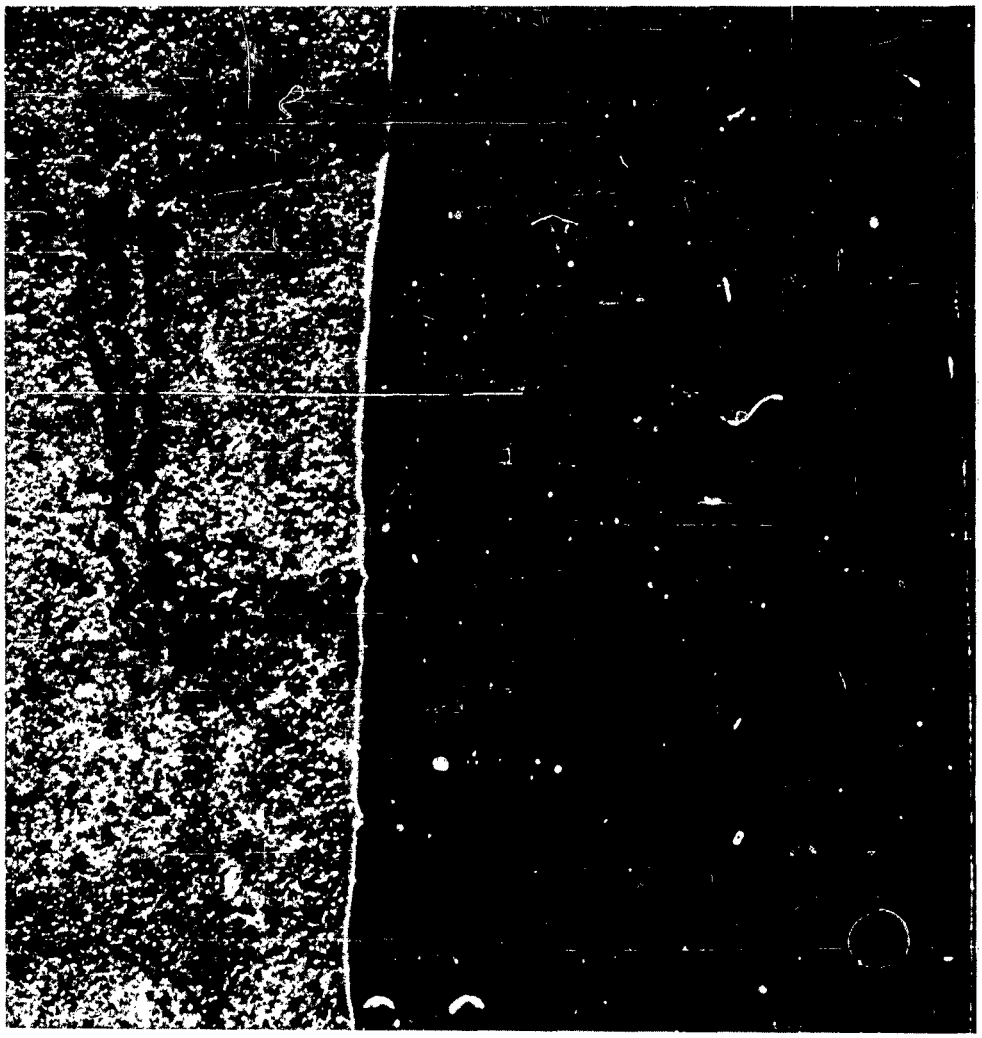

Figure 18. Photomicrograph of the surface of Type "C" conductive glass with a resistance of 9 ohms/square. The bus-bar material is to the left; the resistance surface is to the right. The light line in the center of the photograph is the line of demarkation between film and bus bar.

Appendix B

DEVELOPMENT OF SURFACE THICKNESS AND RESISTIVITY OF FILMS

For metallic films only a few atomic layers thick, the conductivity drops below that of the bulk material. The hypothesis that has been put forward for this drop in conductivity is that the mean free path of the conducting electrons is shortened by collision with the boundaries of the film. For a film thickness[8] greater than about 0.1 of a mean free path, the conductivity can be considered that of the bulk material. For alkali metals the mean free path is approximately 1450 Angstroms, so that a film thickness greater than 145 Angstroms can be considered to have the bulk conductivity value. Commercial metallic films[2] deposited on glass substrata are on the order of 4×10^{-5} inches or $\approx 10^4$ Angstroms thick.

The film can be represented as a surface of thickness t with length Δ and width w. The conductivity is $\sigma_f = \Delta/Rwt$. It is convenient to define surface resistivity as $R_s = R(\Delta/w)$, so that $\sigma_f = 1/R_s t$. For a low surface resistance (10 ohms/square) and a thickness of 4×10^{-2} mils, the conductivity is

$$\sigma_f = \frac{1}{10 \times 4 \times 10^{-2} \times 2.54 \times 10^{-2} \times 10^{-3}}$$

$$\cong \frac{1}{10^{-5}} = 10^5 \text{ mho/meter}$$

The texture of the surface of the two samples was examined under a microscope with magnification of 100. A photomicrograph of two types are shown. The photographed portion of the sample is shown in the sketch below. Figure 18 shows the surface of a 9-ohm/square sample where the film is basically a thin layer of gold which can be applied to plastics as well as glass. Figure 19 shows the surface of a 70-ohm/square sample where the film has been fired into the glass substratum.

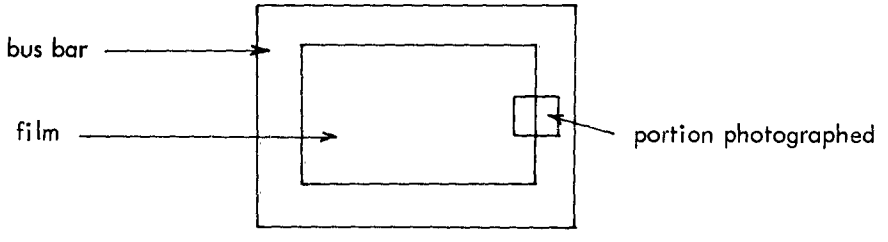

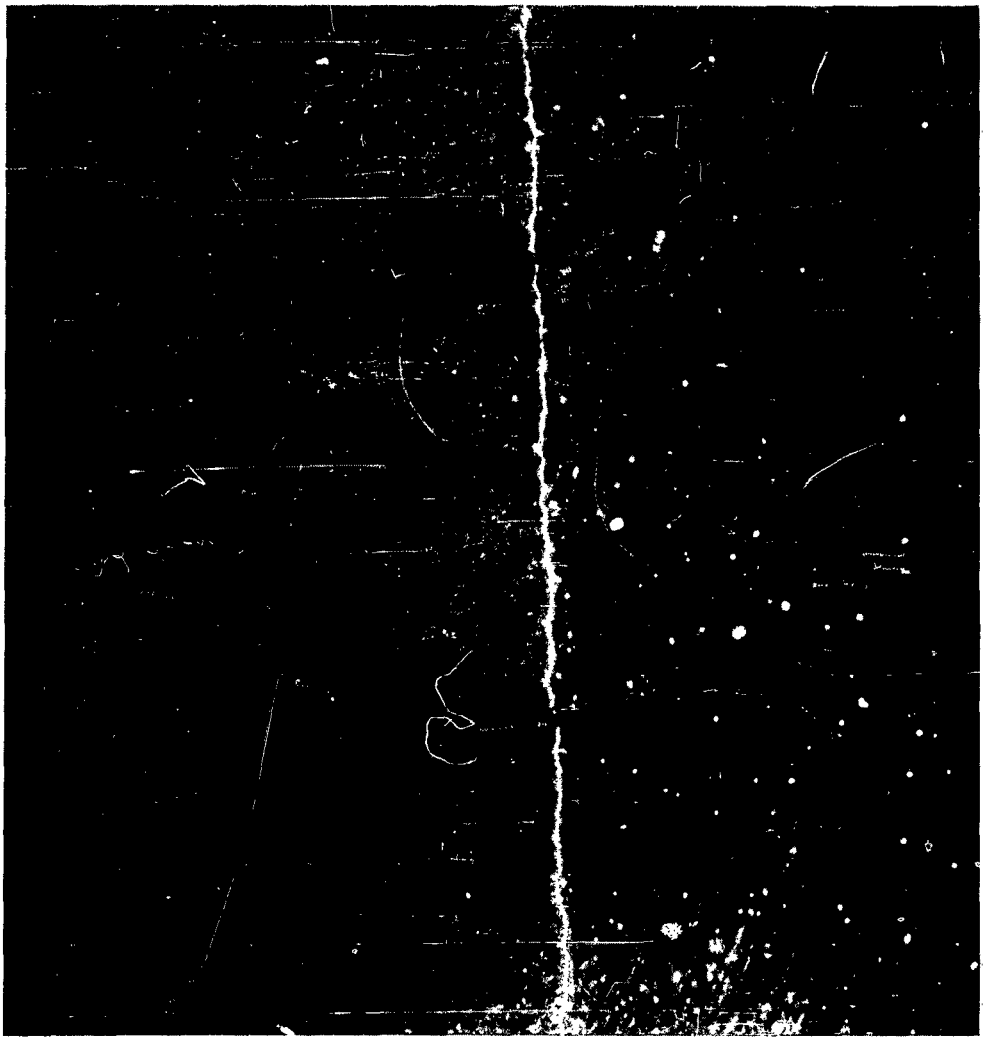

Figure 19. Photomicrograph of the surface of Type "A" conductive glass with a resistance of 70 ohms/square. The junction between the conductive surface and the peripheral bus bar is indicated by the irregular line approximately in the center of the photograph. To the right is the surface of the film and to the left is the bus bar.

DISTRIBUTION LIST

SNDL Code	
	Chief, Bureau of Yards and Docks (Code 70)
23A	Naval Forces Commanders (Taiwan Only)
39B	Construction Battalions
39D	Mobile Construction Battalions
39E	Amphibious Construction Battalions
39F	Construction Battalion Base Units
A2A	Chief of Naval Research - Only
A3	Chief of Naval Operation (OP-07, OP-04)
A5	Bureaus
B3	Colleges
E4	Laboratory ONR (Washington, D. C. only)
E5	Research Office ONR (Pasadena only)
E16	Training Device Center
F9	Station - CNO (Boston; Key West; San Juan; Long Beach; San Diego; Treasure Island; and Rodman, C. Z. only)
F17	Communication Station (San Juan; San Francisco; Pearl Harbor; Adak, Alaska; and Guam only)
F41	Security Station
F42	Radio Station (Oso and Cheltanham only)
F48	Security Group Activities (Winter Harbor only)
H3	Hospital (Chelsea; St. Albans, Portsmouth, Va; Beaufort; Great Lakes; San Diego; Oakland; and Camp Pendleton only)
H6	Medical Center
J1	Administration Command and Unit - BuPers (Great Lakes and San Diego only)
J3	U. S. Fleet Anti-Air Warfare Training Center (Virginia Beach only)
J4	Amphibious Bases
J19	Receiving Station (Brooklyn only)
J34	Station - BuPers (Washington, D. C. only)
J37	Training Center (Bainbridge only)
J46	Personnel Center
J48	Construction Training Unit
J60	School Academy
J65	School CEC Officers
J84	School Postgraduate
J90	School Supply Corps
J95	School War College
J99	Communication Training Center
L1	Shipyards

Distribution List (Cont'd)

SNDL Code	
L7	Laboratory - BuShips (New London; Panama City; Carderock; and Annapolis only)
L26	Naval Facilities - BuShips (Antigua; Turks Island; Barbados; San Salvador; and Eleuthera only)
L30	Submarine Base (Groton, Conn. only)
L32	Naval Support Activities (London & Naples only)
L42	Fleet Activities - BuShips
M27	Supply Center
M28	Supply Depot (Except Guantanamo Bay; Subic Bay; and Yokosuka)
M61	Aviation Supply Office
N1	BuDocks Director, Overseas Division
N2	Public Works Offices
N5	Construction Battalion Center
N6	Construction Officer-in-Charge
N7	Construction Resident-Officer-in-Charge
N9	Public Works Center
N14	Housing Activity
R9	Recruit Depots
R10	Supply Installations (Albany and Barstow only)
R20	Marine Corps Schools, Quantico
R64	Marine Corps Base
R66	Marine Corps Camp Detachment (Tengan only)
W1A1	Air Station
W1A2	Air Station
W1B	Air Station Auxiliary
W1C	Air Facility (Phoenix; Monterey; Oppama; Naha; and Naples only)
W1E	Marine Corps Air Station (Except Quantico)
W1H	Station - BuWeps (Except Rota)
	Deputy Chief of Staff, Research and Development, Headquarters, U. S. Marine Corps, Washington, D. C.
	President, Marine Corps Equipment Board, Marine Corps School, Quantico, Va.
	Chief of Staff, U. S. Army, Chief of Research and Development, Department of the Army, Washington, D. C.
	Office of the Chief of Engineers, Assistant Chief of Engineering for Civil Works, Department of the Army, Washington, D. C.
	Chief of Engineers, Department of the Army, Attn: Engineering R & D Division, Washington, D. C.
	Chief of Engineers, Department of the Army, Attn: ENGCW-OE, Washington, D. C.
	Library of Congress, Washington, D. C.

Distribution List (Cont'd)

SNDL Code	
L7	Laboratory - BuShips (New London; Panama City; Carderock; and Annapolis only)
L26	Naval Facilities - BuShips (Antigua; Turks Island; Barbados; San Salvador; and Eleuthera only)
L30	Submarine Base (Groton, Conn. only)
L32	Naval Support Activities (London & Naples only)
L42	Fleet Activities - BuShips
M27	Supply Center
M28	Supply Depot (Except Guantanamo Bay; Subic Bay; and Yokosuka)
M61	Aviation Supply Office
N1	BuDocks Director, Overseas Division
N2	Public Works Offices
N5	Construction Battalion Center
N6	Construction Officer-in-Charge
N7	Construction Resident-Officer-in-Charge
N9	Public Works Center
N14	Housing Activity
R9	Recruit Depots
R10	Supply Installations (Albany and Barstow only)
R20	Marine Corps Schools, Quantico
R64	Marine Corps Base
R66	Marine Corps Camp Detachment (Tengan only)
W1A1	Air Station
W1A2	Air Station
W1B	Air Station Auxiliary
W1C	Air Facility (Phoenix; Monterey; Oppama; Naha; and Naples only)
W1E	Marine Corps Air Station (Except Quantico)
W1H	Station - BuWeps (Except Rota)
	Deputy Chief of Staff, Research and Development, Headquarters, U. S. Marine Corps, Washington, D. C.
	President, Marine Corps Equipment Board, Marine Corps School, Quantico, Va.
	Chief of Staff, U. S. Army, Chief of Research and Development, Department of the Army, Washington, D. C.
	Office of the Chief of Engineers, Assistant Chief of Engineering for Civil Works, Department of the Army, Washington, D. C.
	Chief of Engineers, Department of the Army, Attn: Engineering R & D Division, Washington, D. C.
	Chief of Engineers, Department of the Army, Attn: ENGCW-OE, Washington, D. C.
	Library of Congress, Washington, D. C.

Distribution List (Cont'd)

Director, U. S. Army Engineer Research and Development Laboratories, Attn: Information Resources Branch, Fort Belvoir, Va.

Headquarters, Wright Air Development Division, (WWAD-Library), Wright-Patterson Air Force Base, Ohio

Headquarters, U. S. Air Force, Directorate of Civil Engineering, Attn: AFOCE-ES, Washington, D. C.

Commanding Officer, U. S. Naval Construction Battalion Center, Port Hueneme, Calif., Attn: Materiel Dept., Code 140

Deputy Chief of Staff, Development, Director of Research and Development, Department of the Air Force, Washington, D. C.

Director, National Bureau of Standards, Department of Commerce, Connecticut Avenue, Washington, D. C.

Office of the Director, U S. Coast and Geodetic Survey, Washington, D. C.

Armed Services Technical Information Agency, Arlington Hall Station, Arlington, Va.

Director of Defense Research and Engineering, Department of Defense, Washington, D. C.

Director, Division of Plans and Policies, Headquarters, U. S. Marine Corps, Washington, D. C.

Director, Bureau of Reclamation, Washington, D. C.

Commanding Officer, U. S. Navy Yards and Docks Supply Office, U. S. Naval Construction Battalion Center, Port Hueneme, Calif.

Facilities Officer (Code 108), Office of Naval Research, Washington, D. C.

Federal Aviation Agency, Office of Management Services, Administrative Services Division, Washington, D. C., Attn: Library Branch

Electronics Branch, Material Laboratory, U. S. Naval Shipyard, Brooklyn, N. Y.

Aeronautical Electronic and Electrical Laboratory, Naval Air Development Center, Johnsville, Pa.

Headquarters, U. S. Air Force Security Service, San Antonio, Tex., Attn: Assistant Director Maintenance and Plant Engineering, DCS/Communications-Electronics

Commanding Officer and Director, U. S. Army Electronic Proving Ground, Fort Huachuca, Ariz.

Mr. Leonard Thomas, Bureau of Ships, Code 695-B, Department of the Navy, Washington, D. C.

Mr. Guy Johnson, Communications Department, U. S. Army Signal Research Development Laboratory, Fort Monmouth, N. J.

Mr. J. Fred Chappel, Communications Department, U. S. Army Signal Research Development Laboratory, Fort Monmouth, N. J.

Mr. Harold C. Hurlbut, Department of the Navy, Northwest and Alaskan Division, Bureau of Yards and Docks, 1638 West Lawton Way, Seattle, Wash.

Mr. A. Goutos, Headquarters, European GEEIA (AFLC), United States Air Force, APO 332, New York

Mr. Paul Wilson, INTEALAB, 150 Causeway Street, Boston

Mr. Rexford Daniels, Interference Consultants, 150 Causeway Street, Boston

Mr. J. Roberts Britton, Chairman, Interference Committee (CIC), The Hawaiian Electric Company Limited, Box 2750, Honolulu

Dr. Ralph M. Showers, The Moore School of Electrical Engineering, University of Pennsylvania, Philadelphia, Pa.

Mr. Fred J. Nichols, Genistron, Incorporated, 6320 West Arizona Circle, Los Angeles

Mr. Don Radmacher, Stoddart Aircraft Radio Corporation, 6644 Santa Monica Boulevard, Hollywood, Calif.

Mr. William Wu, Panoramic Electronics, 520 South Fulton Avenue, Mount Vernon, N. Y.

Mr. William E. Pakala, Westinghouse Research Laboratories, Pittsburgh

U. S. Naval Civil Engineering Laboratory
Technical Report R-242
LOW-FREQUENCY SHIELDING EFFECTIVENESS OF CONDUCTIVE GLASS, by H. A. Lasitter
41 p. illus 20 May 63 UNCLASSIFIED

An evaluation of the electromagnetic-shielding effectiveness of conductive glass.

1. Conductive Glass — Low-frequency shielding effectiveness
I. Lasitter, H. A.
II. Y-F006-09-206

U. S. Naval Civil Engineering Laboratory
Technical Report R-242
LOW-FREQUENCY SHIELDING EFFECTIVENESS OF CONDUCTIVE GLASS, by H. A. Lasitter
41 p. illus 20 May 63 UNCLASSIFIED

An evaluation of the electromagnetic-shielding effectiveness of conductive glass.

1. Conductive Glass — Low-frequency shielding effectiveness
I. Lasitter, H. A.
II. Y-F006-09-206

U. S. Naval Civil Engineering Laboratory
Technical Report R-242
LOW-FREQUENCY SHIELDING EFFECTIVENESS OF CONDUCTIVE GLASS, by H. A. Lasitter
41 p. illus 20 May 63 UNCLASSIFIED

An evaluation of the electromagnetic-shielding effectiveness of conductive glass.

1. Conductive Glass — Low-frequency shielding effectiveness
I. Lasitter, H. A.
II. Y-F006-09-206

U. S. Naval Civil Engineering Laboratory
Technical Report R-242
LOW-FREQUENCY SHIELDING EFFECTIVENESS OF CONDUCTIVE GLASS, by H. A. Lasitter
41 p. illus 20 May 63 UNCLASSIFIED

An evaluation of the electromagnetic-shielding effectiveness of conductive glass.

1. Conductive Glass — Low-frequency shielding effectiveness
I. Lasitter, H. A.
II. Y-F006-09-206